Archives of Microbiology (2022) 204:2
https://doi.org/10.1007/s00203-021-02600-3

ORIGINAL PAPER

Degradation activity of fungal communities on avocado peel (*Persea americana* Mill.) in a solid-state process: mycobiota successions and trophic guild shifts

Patricia Alejandra Becerra-Lucio[1] · Natalia Ysabel Labrín-Sotomayor[1] · Max Mizraím Apolinar-Hernández[2] · Angel Antonio Becerra-Lucio[1] · José E. Sánchez[3] · Yuri Jorge Peña-Ramírez[1]

Received: 15 July 2020 / Revised: 19 November 2021 / Accepted: 21 November 2021 / Published online: 4 December 2021

Abstract

To explore the capability of soil mycobiota to degrade avocado peel waste and identify relevant successions and trophic guild shifts, fungal communities from three environments with different land uses were evaluated in a solid-state process. Soil samples used as inoculum were collected from a pristine mature tropical forest, a traditionally managed Mayan land, and an intensively managed monospecific avocado plantation. Soil-substrate mixes were evaluated for 52 weeks to evaluate organic matter decay and the carbon-to-nitrogen ratio. Amplicon-based high-throughput sequencing from internally transcribed spacer (ITS) analysis revealed significant differences in fungal communities widely dominated by *Fusarium* sp. and *Clonostachys* sp.; however, less represented taxa showed relevant shifts concomitantly with organic matter content drops. Trophic guild assignment revealed different behaviors in fungal communities between treatments over the 52 weeks, suggesting distinct preconditioning of fungal communities in these environments. Overall, the results lead to the identification of promising degradation moments and inoculum sources for further consortia enrichment or bioprospecting efforts.

Keywords Land-use impact · Tropical forest · Gadgil effect

Introduction

The avocado (*Persea americana* Mill. [Lauraceae]) is one of the most important fruit crops in the world, with Mexico being the world's largest producer (FAO 2021). Enormous amounts of peel waste present important challenges for processing and exploitation (Araújo et al. 2018). Lignocellulosic waste, such as avocado peel, is decomposed by biological degradation carried out mainly by wood-rotting fungi: Basidiomycetes (white- and brown-rot fungi that preferentially degrade lignin, cellulose, and hemicelluloses), some Ascomycetes (white rot), Deuteromycetes, Aspergillus niger, Trichoderma reesei (soft-rot fungi), and anaerobic (rumen) fungi (Madadi and Abbas 2017). Soil associated with wood decay, particularly those associated with white rot, has been used since early last century as a source for the isolation and study of fungal communities to improve degradation processes (Leutritz Jr 1946). In regard to soil isolates, the identification of highly effective consortia has considered rich environments such as pristine tropical forest soils, where the decay process of a multitude of vegetal species is related to hotspots of fungal diversity (Husband et al. 2002). However, pristine tropical forests showed a slower decomposition rate than monospecific managed lands (McGuire et al. 2010). The use of mechanization, manure, irrigation, agrochemicals, and other practices alters microbial diversity, abundance, and biological activity (Yao et al. 2000). These factors may disrupt the spatial relations between symbiotrophs, saprotrophs, and pathotrophs

Communicated by Erko Stackebrandt.

✉ Yuri Jorge Peña-Ramírez
ypena@ecosur.mx

[1] Department of Sustainability Sciences, El Colegio de la Frontera Sur Unidad Campeche, Av. Rancho Polígono 2-A Col. Ciudad Industrial, CP 24500 Lerma, Campeche, Campeche, Mexico

[2] Institute of Biotechnology, Department of Biological Sciences, Universidad Autónoma de Nuevo León, Av. Universidad s/n. Ciudad Universitaria, CP 66455 San Nicolás de los Garza, Nuevo León, Mexico

[3] Department of Sustainability Sciences, El Colegio de la Frontera Sur Unidad Tapachula, Carretera Antiguo Aeropuerto km 2.5, CP 30700 Tapachula, Chiapas, México

(Fernandez and Kennedy 2016), increasing the relative abundance of certain guilds, such as rot-related saprotroph fungi (Maaroufi et al. 2019). This alteration, known as the "Gadgil effect" (Fernandez and Kennedy 2016), was first described in soil forests. Similar mycobiota structure shifts in response to substrate changes, increasing relative abundance levels of saprotrophs, and concomitant reductions in symbiotrophs such as ectomycorrhizal representatives have been consistently reported in plant waste fermentation processes (Zhang et al. 2016). This successional phenomenon has been used to explore degrading-consortia enrichment (Jiménez et al. 2014b; de Lima Brossi et al. 2016). Thus, we hypothesize that the use of managed soils as an inoculum source for lignocellulosic degradation processes may be advantageous, because in these environments, the soil microbiota is expected to be prone to higher degradation efficiency. Soil management intensity should play a crucial role when used as an inoculum source; however, intensive management differs from traditional management. The Mayan families in Mesoamerica typically maintain an agricultural self-consumption backyard area, harboring high biodiversity composed of native and exotic crops, trees, livestock, and wild fauna (Montagnini 2006). Following this reasoning, we focus on two questions: Do the fungal communities present in pristine, backyard, and intensive soil sources show similar degradation capabilities on avocado peel in a solid-state process? Do fungal communities from pristine and managed environments show similar structure shifts and trophic guild compositions during this process? To address these questions, we evaluated changes in mycobiota compositions and guild balances using soil from pristine Mayan forests, traditional Mayan backyards, and intensively managed avocado commercial orchards during avocado peel degradation as an inoculum source. Solid-state degradation was selected due to previously reported advantages regarding taxon representativeness (Hölker et al. 2004); furthermore, similar mycobiota shift evaluations in solid-state systems confirmed its feasibility (Cerda et al. 2017).

Materials and methods

Collection of microbial and substrate inocula

Soil used as inoculum was collected from three environments with different land uses: pristine, backyard, and intensive. The soil samples were collected from the following locations: a) pristine, mature, > 150-year-old, midelevation evergreen forest in Calakmul, Campeche, Mexico (18° 9′ 48″ N; 89°23′ 53″ W) previously described by García-Licona et al. (2014) and considered the best conserved environment of the original distribution of *Persea americana* in the northern neotropics (Galindo-Tovar et al. 2007); b) backyard, a typical ~ 50-year-old traditional Mayan family backyard described Montagnini (2006) located in Kobén, Campeche, Mexico (19° 55′ 02″ N; 90° 24′ 57″ W); and c) intensive, ~ 30-year-old orchard monoculture of *P. americana* var. Hass managed with a technological package, including mechanization, the use of synthetic fertilizers, pesticides, and herbicides, located in San Juan Nuevo Parangaricutiro, Michoacán, Mexico (19° 25′ 09″ N; 102° 08′ 14″ W). In each location, three sampling points 50 m away each were randomly selected, which were located 1 m away from mature healthy trees by their typical representative aspects (*Licaria* sp. [Lauraceae] in pristine and *P. americana* in Backyard and Intensive sites). The soil was collected in the first 15 cm of depth and mixed to form a composite sample of approximately 1.5 kg per site; the composite samples were transferred into plastic bags in a cooler at 4 °C (8 h max), aseptically milled, sieved through a 40-gauge mesh, and immediately used for substrate inoculation. Proximal analysis of composite soil samples is presented in Supplementary File SF2.

Substrate preparation

Peels of overripe fruits from a commercial harvest of avocado *P. americana* var. Hass substrate were used. The peel was cleaned by removing the pulp and pit and rinsing it thoroughly with water. Dried husk was aseptically pulverized in a manual mill. The resulting powder was sieved through a 40-gauge mesh and autoclaved at 121 °C (1.05 kg·cm^{-2}) for 20 min. Subsequently, it was dried aseptically in a natural convection oven at a constant temperature of 70 °C for 72 h. The resulting avocado flour composed of approximately [acid-insoluble lignin 35.0%; polymeric sugars 23.6%; aqueous extractives 15.5%; and lipids and protein < 6% (García-Vargas et al. 2020)] was used as the sole external substrate.

Solid-state degradation

The bioassay for each treatment was conducted in a dry, static, sterile 2-L plastic polypropylene large-wide mouth round bottle (2121-series Nalgene) and established in triplicate by a mix of a 3:1 substrate:inoculum (w/w) ratio (1.2 kg total). Containers were set at room temperature (~ 24 °C) with manual, vigorous homogenization shaking every 2 days and monitored for 52 weeks. During the incubation period, samples from each treatment were obtained at 0, 4, 8, 12, 16, 24, and 52 weeks under aseptic conditions in a flow chamber. A sample at time zero was obtained immediately after the mix was set. Each sample consisted of material taken from every repetition (previous brief shaking); 1 g for DNA extraction, 1 g for carbon-to-nitrogen (C/N) ratio determination, 100 g for OM analysis, and 100 g for other experiments were placed in conical 50-mL tubes, frozen

with liquid nitrogen, and stored in a deep freezer at -70 °C for further analysis.

Sequencing the internally transcribed spacer (ITS) region

Total genomic DNA was extracted from 250 mg of each sample with the "PowerSoil™ DNA Isolation Kit" (M/s MoBio, Carlsbad, CA, US) following the manufacturer's instructions. DNA concentration and purity determination were performed by spectrophotometry on the Multiskan GO® model FI-01620 with µDrop Plate and SkanIt® software, version 4.1 (M/s Thermo Scientific, Waltham, MA, US). Ten nanograms of DNA of each repetition per sample was pooled and sequenced using the MiSeq® Illumina 2000 platform in Research and Testing Laboratories (RTL Genomics www.rtlgenomic.com). The oligonucleotides used for sequencing were ITS1 (Fw 5' TCCGTAGGTGAACCT GCGG 3') and ITS4 (Rv 5' TCCTCCGCTTATTGATATGC 3') (Voříšková and Baldrian 2013).

Bioinformatic analysis

The raw sequencing data were obtained from RTLGenomics (www.rtlgenomic.com) as *.fastq files available through the NCBI (Accession number PRJNA625561) and were quality analyzed using the MultiQC report (Ewels et al. 2016) and processed using the QIIME 2 suite (Bolyen et al. 2019) following the ITSxpress pipeline developed by Rivers et al. (2018) (Supplementary File SF1). Taxonomy was assigned according to the UNITE Taxonomy Dataset, version 18.11.2018 (UNITE Community 2019). Functional trophic guilds of OTUs were assigned using the FUNGuild annotation tool (Nguyen et al. 2016) running the *Guilds_v1.1.py* script locally, which is available through https://github.com/UMNFuN/FUNGuild.

Organic matter and carbon-to-nitrogen ratio determination

For each sample, the organic matter (OM) content was quantified by the combustion method at 550 °C for 2.5 h in a muffle. The C/N ratio was determined by automated analysis; 2 mg of each sample (quintupled) was passed through a sieve and analyzed with a Perkin-Elmer CHNO/S 2400 instrument (Waltham, MA, US) following the manufacturer's instructions.

Statistical analysis

One-way analysis of variance with Duncan's test was used to identify treatment differences at $P < 0.05$ for the C/N ratio passing the assumption tests. Correlation analysis (using Pearson's coefficient) was performed to determine the relationship between fungal populations at the genus level, trophic guilds, and soil parameters. All these analyses were performed using InfoStat for Windows software (https://www.infostat.com.ar/). The output of the crude analysis is provided in Supplementary File SF3.

Results

Organic matter and carbon-to-nitrogen ratio analysis

As a first approach to monitoring solid-state fermentation over time, the OM content was determined in the three different treatments for 52 weeks. After each substrate-soil mix was set, the starting OM content was determined for the pristine (34.8%), intensive (33.1%), and backyard (24.1%) treatments. During fermentation, the OM in the substrate mix decayed over time, showing significant differences ($P < 0.05$) among the treatments. The relative loss of OM showed a biphasic curve in all treatments (Fig. 1a). Data were best fitted to a third-grade polynomic model resulting in higher R^2 values compared to other models, including the backyard treatment, where data fitting to a linear model was slightly lower ($R^2 = 0.9647$). In all cases, the first degradation round occurred between weeks 4 and 12, and a second round, which was less drastic, was detected between weeks 18 and 52. At the end of the experiment, the greatest relative OM loss was detected in the intensive treatment (76%), followed by the backyard (42%) and pristine (39%) treatments. The C/N ratio was also calculated for the same samples except for 52-week samples (Fig. 1b). After inoculation, the C/N ratios in the substrate mix for the pristine treatment were significantly higher (36.1) than the values detected in the backyard (26.6) and intensive (25.1) treatments. During the following weeks of fermentation, the C/N ratios from the pristine and backyard treatments followed a decay pattern; in contrast, the intensive treatment showed different behavior, with two peaks of the C/N ratio detected at weeks 8 and 18. The observed differences in the C/N ratio were significantly different ($P < 0.05$) for both treatments and weeks of sampling, with the exception of week 8; furthermore, a significant correlation between OM and C/N ratio decay was also observed at the same significance level according to the Pearson coefficient (Supplementary File SF3).

General analysis of the fungal communities

To evaluate the fungal communities putatively responsible for the degradation activity, metagenomic analysis of the samples resulted in a total of 1,076,420 sequences of the ITS region obtained from the 21 composite samples (7 sampling

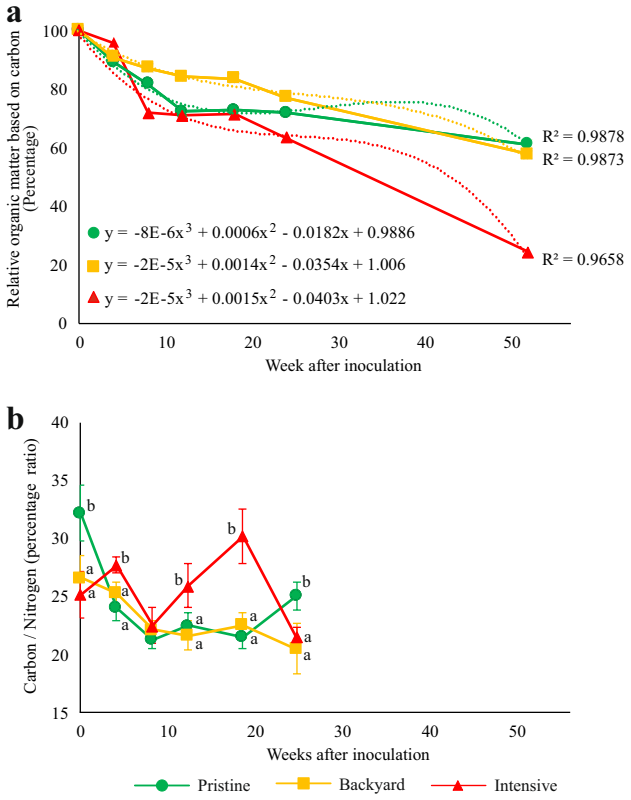

Fig. 1 Carbon decay during solid-state fermentation. Organic matter (OM) content (**a**) and carbon/nitrogen ratio decay (**b**) measured during fermentation. OM was determined as a composite sample corresponding to each repetition ($n=3$); the C/N ratio was determined individually for each repetition; error bars correspond to standard deviations, and different letters next to error bars correspond to significant differences. The C/N ratios at 52 weeks were not determined

times per treatment; three repetitions), showing an average read length of 229.4 bp. Trimmed sequences resulted in the identification of 157 OTUs, 5 phyla, 12 classes, 26 orders, 48 families, 78 genera, and 85 species, leaving 45% unidentified species. The rarefaction curves of the 21 samples revealed that the fungal communities were well represented at the 6,667-read cutoff level, and the data show that phylotype richness, ranging from 20 to 65 OTUs, reached a steady trend in all of the samples (Supplementary File SF4). The fungal relative abundance at the species level illustrated in the bar plot (Fig. 2) revealed that the soil communities from the three inocula (time zero) were quite different and were clearly dominated by *Funneliformis* sp., and *Aspergillus* sp. in the pristine and backyard provenances, respectively, whereas for the intensive treatment, the fungal community present in the inocula consisted of a heterogeneous community dominated by four different phylotypes belonging to the *Ascomycota* phylum, all of which were distinct from those dominating the pristine and backyard soils. In all the treatments, the initial communities showed important shifts over the 52 weeks of solid-state fermentation. For the pristine treatment, changes in relative abundance were detected by week 4, tending to maintain the abundance of *Fusarium solani*, with the enrichment and maintenance of *Fusarium keratoplasticum* by week 52. For the backyard treatment, a profound shift was observed by week 4 with a strong decay of *Aspergillus* sp. (barely recovered by week 24) and dominated by *Fusarium solani*. In the intensive treatment, the shifts were subtle, with the dominance of the original phylotypes maintained over the 52 weeks. All the treatments were dominated by *Ascomycota* representatives, and in all the treatments, the presence of minority species was detected, some of which were exclusive to each treatment. In the bar plot, some of these species can be identified, such as *Clonostachys compactiuscula* or *Cutaneotrichosporon smithiae,* as examples of phylotypes representing > 1% of the sample exclusively in the pristine, backyard, or intensive treatment, respectively.

Clustering analysis of fungal communities

To perform a more detailed analysis of the composition of the communities, a hierarchically clustered heatmap at the genus level was generated based on the Euclidean coefficient of association (Fig. 3). Sample analysis revealed the formation of three major clusters based on the similarity of fungal community structures. These clusters matched the three treatments, grouping clusters from the pristine and backyard treatments together and leaving separate the third cluster belonging to the intensive treatment. Within the treatments, early samples (0, 4, and 8 weeks) were clustered together in all cases. Clustering analysis with respect to microbial diversity resulted in the formation of two major groups: the first was a discrete group (Fig. 3, cluster C1) composed of the three highly represented phylotypes belonging to the *Hypocreales* order, and the second large group represented the less frequent phylotypes. A detailed examination led to the identification of microorganisms mostly or exclusively detected in the pristine, backyard, or intensive treatment (Fig. 3, clusters P, B, and I, respectively; Supplementary File SF5), as well as some clusters present only during weeks 4–12 in the pristine and intensive treatments (Fig. 3, cluster D), corresponding to the strongest decay rates detected in these treatments.

Diversity analysis

Alpha diversity in samples along solid-state fermentation time courses was determined at the species level. The observed OTUs and Chao, Shannon, and Simpson diversity indices were calculated (Supplementary File SF6). Values derived from the Shannon index suggested that fungi from the three treatment communities harbor moderate-to-high

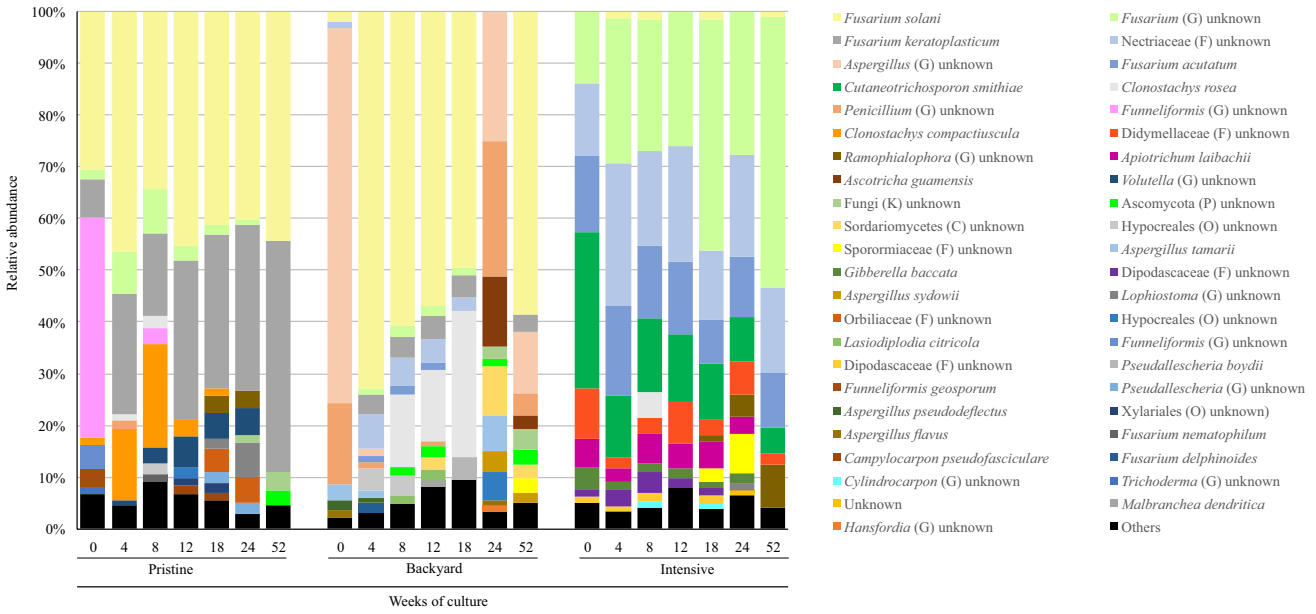

Fig. 2 Fungal relative abundance across fermentation. Dominant phylotypes representing ≥ 1% per sample at the species level. Unknown and unassigned clades are presented as the immediate taxonomy match at the G, genus; F, family; O, order; C, class; P, phylum; and K, kingdom levels. Less represented phylotypes are grouped as "others." Each bar corresponds to a composite sample consisting of three repetitions

diversity through degradation kinetics. Simpson index values suggest that communities with similar degrees of dominance appear consistently in the backyard community. Time zero samples, corresponding to the soil microbial structure in the three environments, revealed significantly greater diversity in the pristine and intensive treatments than in the backyard treatment. However, after the first weeks of fermentation, statistically significant shifts in diversity index values were consistently observed, showing drastic variations between weeks 4 and 12. In contrast, regarding beta diversity, Euclidian correlation analysis showed significant differences between fungal communities present in the three treatments, and these differences were maintained over the 52 weeks of fermentation.

Trophic guild analysis

The obtained phylotypes were arranged by their relative abundance levels by trophic guilds during the degradation process (Fig. 4). In the pristine treatment, time zero communities were almost equally represented, and symbiotrophs were slightly more abundant, followed closely by pathotrophs and saprotrophs. However, after 4 weeks of degradation, this pattern reversed drastically, ending by week 52 with relative abundance levels greater than 45% for pathotrophs and saprotrophs and only nearly 5% for symbiotrophs. For the backyard treatment, initial relative abundance levels were also balanced, with the saprotroph abundance being the highest, followed closely by the other two groups. In this treatment, a similar pattern was found, and after 4 weeks, pathotrophs and saprotrophs significantly increased their abundance levels, whereas the symbiotrophs abundance dropped to nearly 10%. Finally, for the intensive treatment, the initial abundance was clearly dominated by pathotrophs, followed by saprotrophs and symbiotrophs. In this case, after 4 weeks and until the end of the experiment, all the groups' abundance levels tended toward a balance, culminating in values of approximately 31–34% by week 52. Furthermore, statistical analysis revealed significant differences ($P < 0.05$) in trophic guild populations by treatment and a strong, negative, significant positive correlation ($P < 0.05$) between saprotrophs and OM in the pristine and intensive treatments, as well as among pathotrophs, OM, and the C/N ratio in the pristine treatment, and a significant negative correlation ($P < 0.05$) between saprotrophs and symbiotrophs.

Discussion

The successful finding of novel degrading fungal consortia mostly depends on the selection of an adequate environmental sample. Bioprospecting efforts may be worthless if incorrect samples are analyzed, resulting in large amounts of data for well-characterized species or poorly represented, and thus undetectable, ITS tags or expressed sequences of interest (Li et al. 2009). As a first step for the selection of

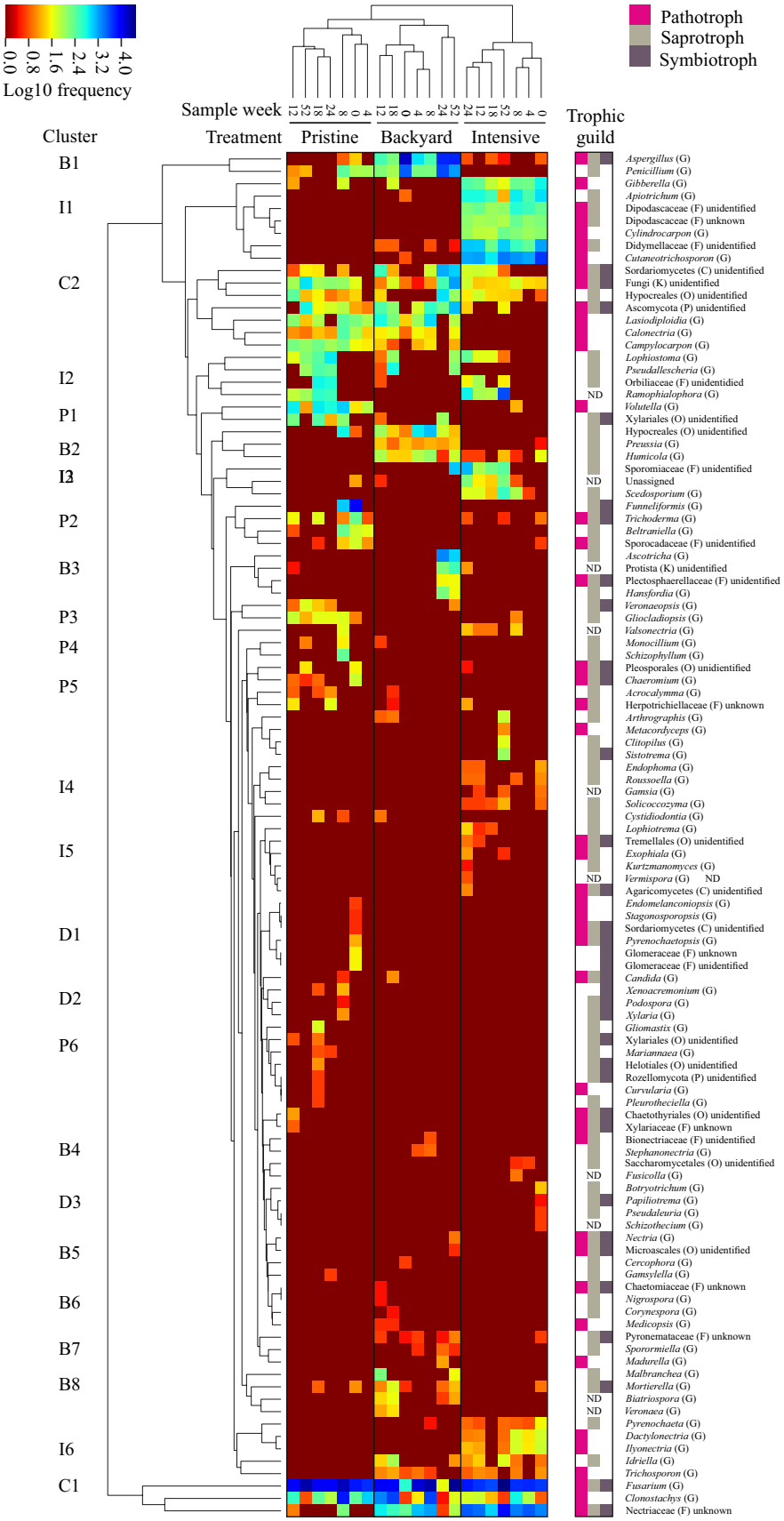

Fig. 3 Abundance heatmap and assigned trophic guilds. Phylotypes at the genus level (G) are plotted according to Jaccard's association coefficient relative to similarities between samples and fungal communities. Unknown and unassigned clades are presented as immediate taxonomy matches at the F, family; O, order; C, class; P, phylum; and K, kingdom levels. Clusters correspond to phylotypes mostly or exclusively present in the pristine, backyard, and intensive treatments (clusters P, B, and I, respectively). D clusters correspond to representatives with increased abundance with simultaneous drastic OM and C/N ratio shifts. Trophic guild assignments are presented in the right box. ND: Not determined

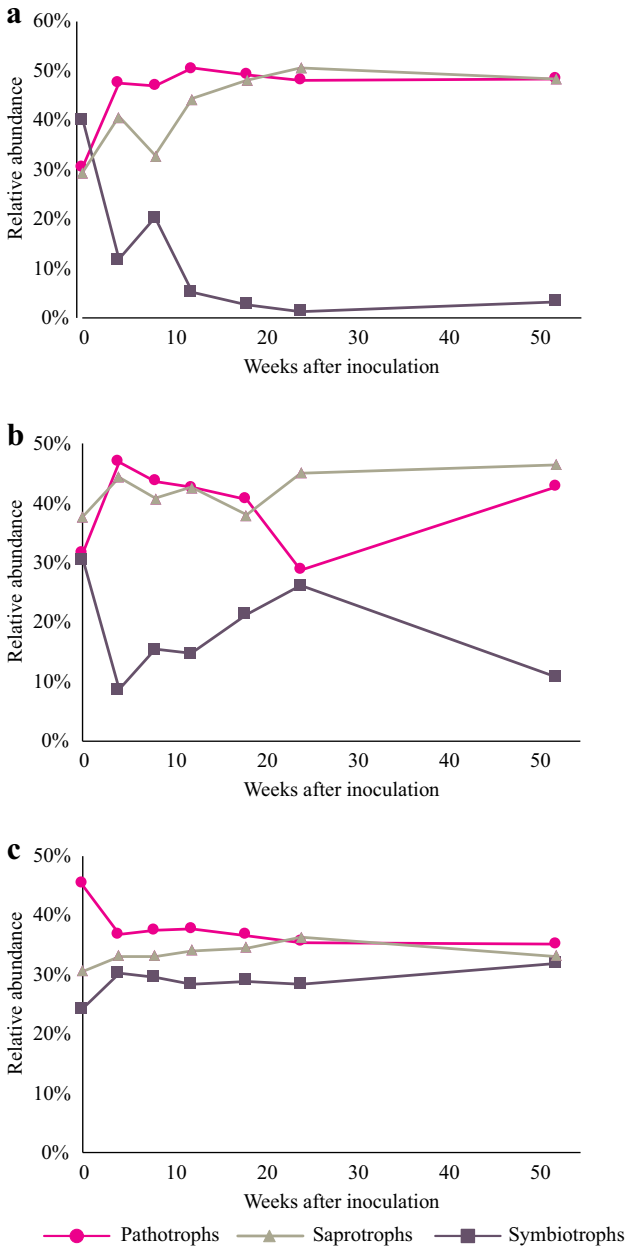

Fig. 4 Trophic guild dominance. Fungal relative abundance levels of phylotypes according to their trophic guild assignments in pristine (**a**), backyard (**b**), and intensive (**c**) treatments

promising samples for the identification of relevant consortia, we employed a solid-state degradation approach to identify the best source of inoculum and the most promising sampling times for the identification of nontraditional fungi associated with avocado peel degradation. OM contents, and C/N ratios were employed as indicators of degradation activity.

Our results showed significant shifts in the OM content and C/N ratio across the 52 weeks evaluated. In this period, the microbial degradation activity showed significant differences among treatments, which were possibly attributable to two factors: 1) the resulting substrate–soil mix at time zero and 2) the composition of microbial communities present in each inoculum. In the first case, considering the composition of avocado peel (see the reference in the M&M section), the microbial communities faced initial substrate conditions richer in OM content (13.4% higher in pristine; 10.2% higher in backyard; and 25.06% higher in intensive sites) than derived soil (Supplementary File SF2), which may explain why pristine and intensive treatments showed higher degradation performance in the first 12 weeks than the backyard treatment. Similar observations have been reported in other solid-state degradation experiments where soil was used as the inoculum source and fungal communities had abundant OM contents (Jiménez et al. 2014a). Our data suggest that the initial decay may be due to rapid degradation of less resilient components in avocado peel, followed by more complex components commonly degraded by rot-associated taxa (Menezes and Barreto 2015). This biphasic polynomial fitting model applied to our data indicates that all treatments followed the same pattern, including the backyard treatment that apparently follows a constant degradation rate. Similarly, the C/N ratios were substantially different in the starting soil–substrate mix in the pristine and backyard treatments (12.16 and 6.15, respectively) in contrast to a slightly higher value in the intensive treatment (0.82). Across the degradation dynamics, all treatments showed a net C/N loss by week 24. Pristine and backyard treatments followed a closer pattern during the kinetics than during the intensive kinetics, which showed two peaks by weeks 4 and 18. These data may indicate an increase in nitrifying activity in this treatment attributable to bacteria; however, this taxon was not considered in this work. Another plausible explanation of the observed behavior relies on the solid-state degradation system employed here. Although the mixes were regularly homogenized, the distinct proportions of loan and clay from soil added to the mix in each treatment may form different microenvironments, biofilms, or chelating conditions altering the availability of micronutrients, oxygen, water, and light for the microbial community (Vassileva et al. 2021).

The obtained data revealed significant differences in fungal structure between treatments. Contrasting diversity at time zero reflects the particular mycobiota structure in the soil used as inoculum in each case. Despite the overwhelming *Fusarium*, *Clonostachys*, and *Nectriaceae* OTU abundance levels in all samples, possibly due to OM present in the soil inoculum (Hubbe et al. 2010), the diversity index values showed that the initial richness was significantly higher in the pristine and intensive treatments than in the backyard treatment. These results are consistent with those of previous reports showing minor impacts on fungal diversity in avocado orchards compared with pristine forests (González-Cortés et al. 2012). During the degradation

dynamics, important shifts in fungal structure and diversity indices were observed in all treatments, as may be expected as a consequence of a drastic environmental and substrate changes. Several groups were initially well represented, such as *Funneliformis* sp. (51%) in the pristine treatment, and *Aspergillus* sp. (72%) in the backyard treatment decreased in relative abundance to levels near or below 1% by week 4. The rapid decrease in dominant taxa in the early degradation dynamics is consistent with previous evidence in other solid-state fermentation systems where the genera *Aspergillus*, *Millerozyma*, *Monascus*, and *Xeromyces* presented drastic drops in their relative abundance associated with substrate changes (Liu et al. 2020). However, in the case of intensive treatment, the mycobiota structure did not vary drastically over the 52 weeks of culture, supporting the preconditioned fungal community idea. This community may be preadapted to *P. americana* lignocellulosic material, where dominating taxa preserve saprotroph guild dominance during all kinetics (Fig. 4c). Euclidean clustering of relative abundance levels in samples led to the identification of taxa highly represented in certain treatments and times but reduced or absent in others. These successions are very common in this kind of degradation dynamics and can be used for the identification of putative consortia specialized in the degradation of primary, secondary, or even tertiary substrates (Liu et al. 2020). In contrast, representatives of the Hypocreales order may not be considered part of specialized consortia, as its abundance did not correlate with OM content decay, guild, or C/N shifts. Hence, the observed differences in decay patterns between treatments may be attributable to particular microbial representatives present in each treatment and moment, such as some members of consortia previously identified during lignocellulosic decay, including *Pyrenochaetopsis* sp. (Zhang et al. 2020), *Podospora* sp. (Couturier et al. 2016), and *Xylaria* sp. (Bittner et al. 2012), and other genera related to plant pathogenesis and wood decomposers, including *Botryotrichum* sp., *Papiliotrema* sp., and *Pseudaleuria* sp. (Cannon and Kirk 2007; Tedersoo et al. 2014; Sterkenburg et al. 2015), most of which appeared in the intensive treatment and may be interesting examples of fermenting fungi commonly isolated from managed soils and agricultural products (Yurkov 2018).

Trophic guild assignments revealed interesting shifts. In the pristine treatment, a drastic reduction in symbiotrophs accompanied by rapid domination of saprotrophs and pathotrophs was observed, indicating the loss of functional symbiotic networks previously maintained in the soil by the vegetal component (Fernandez and Kennedy 2016), which, once absent under the experimental conditions, were rapidly displaced by degrading saprotrophs and pathotroph representatives. In the backyard treatment, the same pattern was observed. Nevertheless, succession events are present even in later samples (weeks 18–52), supporting the idea of a more complex adaptive process with secondary niches formed late in this treatment. Similarly, fungal community shifts in the backyard treatment were constant over the 52 weeks, suggesting a continuous response to changes in the substrate over time as new niches formed that could be occupied by previously less abundant phylotypes (Voříšková and Baldrian 2013). In contrast, for the intensive treatment, no significant guild shift was observed, which might indicate the loss of functional networks in the original environment that maintains the suppression of pathotrophs and saprotrophs, driven perhaps by the external input of nutrients and agricultural disturbances, which may suggest that the Gadgil effect may be lost before sample collection, and present organisms related to other guilds are unable to establish a population balance in intensively managed fields and during the degradation dynamics. In this case, soil from intensive treatment was demonstrated to favor the proliferation of saprotrophs simultaneously with a rapid OM decay in avocado peel waste.

Conclusion

The finding of some phylotypes appearing exclusively in the pristine treatment during the early weeks of fermentation, together with drastic OM and C/N decay and after putative "release" of the Gadgil effect, is particularly interesting. The presence of some genera, such as *Endomelanconiopsis* and *Stagonosporopsis*, the two phylotypes belonging to the Glomeraceae family (pathotrophs guild), and one from the Sordariomycetes class (symbiotrophs guild), suggests that samples obtained during weeks 4–12 are promising for metatranscriptomic or functional searches for lignocellulolytic enzymes. Similarly, in the intensive treatment, some phylotypes appearing exclusively in samples from weeks 8 to 12, when drastic OM and C/N decay were observed, were representative of genera such as *Botryotrichum*, *Papiliotrema*, *Pseudaleuria* (saprotrophs guild), *Schizothecium*, and *Fusicolla* (undetermined guild); in addition, a member of the Saccharomycetales order (saprotrophs guild) became a prominent candidate for subsequent bioprospecting efforts. Finally, for the backyard treatment, the OM and C/N ratio decay were not clear drivers of the decision of which sample might be more relevant. Nevertheless, the balance between trophic guilds suggests two separate moments (weeks 4 and 52) when the Gadgil effect "release" criteria could be applied. In particular, for the last sample, some genera appearing exclusively at this time were *Monocillium, Cystidiodontia, Nigrospora* and a representative of the Orbiliaceae family (saprotroph guild), which also warrants further exploration for novel catalytic activities and regulatory processes for lignocellulosic degradation. All these factors may have contributed to the generation of contrasting conditions

between treatments that generated different fungal populations, presenting the opportunity for deeper studies of the corresponding microbiota.

Supplementary Information The online version contains supplementary material available at https://doi.org/10.1007/s00203-021-02600-3.

Acknowledgements PABL is indebted to Consejo Nacional de Ciencia y Tecnología (CONACYT) for her Master's scholarship, number 624547. YPR thanks Consejo Estatal de Investigación Científica y Desarrollo Tecnológico de Campeche (COESICYDET) for its financial support (2015-2018) and El Colegio de la Frontera Sur for financial support received through research grant 5103711808.

Author contributions All authors contributed to the study conception and design. Material preparation and data collection and analysis were performed by all authors. The first draft of the manuscript was written by YJPR, and all authors commented on previous versions of the manuscript. All authors read and approved the final manuscript.

Funding Consejo Estatal de Investigación Científica y Desarrollo Tecnológico de Campeche (COESICYDET) (2015–2018). El Colegio de la Frontera Sur research grant 5103711808.

Data availability The crude sequence dataset is available under NCBI accession number PRJNA625561. A pipeline for the bioinformatic data process is included in Supplementary File SF1. The samples analyzed may be available upon request after a share transfer agreement. The datasets generated during the current study are available from the corresponding author upon reasonable request.

Declarations

Conflict of interest None.

Ethical approval This work received approval from the Comité de Ética para la Investigación from El Colegio de la Frontera Sur in April 2017. Samples were collected after approval from SEMARNAT according to "Permiso de colecta de material biológico para investigación científica" granted to authors and a previously informed agreement obtained from the Traditional Mayan backyard owner.

References

Araújo RG, Rodriguez-Jasso RM, Ruiz HA et al (2018) Avocado by-products: nutritional and functional properties. Trends Food Sci Technol 80:51–60

Bittner B, Kellner H, Jehmlich N et al (2012) The wood rot ascomycete Xylaria polymorpha produces a novel GH78 glycoside hydrolase that exhibits α-L-rhamnosidase and feruloyl esterase activities and releases hydroxycinnamic acids from lignocelluloses. Appl Environ Microbiol 78:4893–4901

Bolyen E, Rideout JR, Dillon MR et al (2019) Reproducible, interactive, scalable and extensible microbiome data science using QIIME 2. Nat Biotechnol 37:852–857

Cannon PF, Kirk PM (2007) Fungal families of the world. Cabi, Singapore

Cerda A, Gea T, Vargas-García MC, Sánchez A (2017) Towards a competitive solid state fermentation: cellulases production from coffee husk by sequential batch operation and role of microbial diversity. Sci Total Environ 589:56–65. https://doi.org/10.1016/j.scitotenv.2017.02.184

Couturier M, Tangthirasunun N, Ning X et al (2016) Plant biomass degrading ability of the coprophilic ascomycete fungus Podospora anserina. Biotechnol Adv 34:976–983

De MCR, Barreto AR (2015) Biodegradação de resíduos lignocelulósicos por fungos basidiomicetos : Caracterização dos resíduos e estudo do complexo enzimático fúngico. Rev Eletrônica Em Gestão, Educ e Tecnol Ambient 19:1365–1391. https://doi.org/10.5902/2236117016853

de Lima Brossi MJ, Jiménez DJ, Cortes-Tolalpa L, van Elsas JD (2016) Soil-derived microbial consortia enriched with different plant biomass reveal distinct players acting in lignocellulose degradation. Microb Ecol 71:616–627. https://doi.org/10.1007/s00248-015-0683-7

Ewels P, Magnusson M, Lundin S, Käller M (2016) MultiQC: summarize analysis results for multiple tools and samples in a single report. Bioinformatics 32:3047–3048

Fernandez CW, Kennedy PG (2016) Revisiting the 'Gadgil effect': do interguild fungal interactions control carbon cycling in forest soils? New Phytol 209:1382–1394

Galindo-Tovar ME, Arzate-Fernández AM, Ogata-Aguilar N, Landero-Torres I (2007) The avocado (Persea americana, Lauraceae) crop in Mesoamerica: 10,000 years of history. Harvard Pap Bot 12:325–334

García-Licona JB, Esparza-Olguín LG, Martínez-Romero E (2014) Estructura y composición de la vegetación leñosa de selvas en diferentes estadios sucesionales en el ejido El Carmen II, Calakmul, México. Polibotánica 38:1–26

García-Vargas MC, del Contreras M, Gómez-Cruz I et al (2020) Avocado-derived biomass: chemical composition and antioxidant potential. Proceedings 70:100. https://doi.org/10.3390/foods_2020-07750

González-Cortés JC, Vega-Fraga M, Varela-Fregoso L et al (2012) Arbuscular mycorrhizal fungal (AMF) communities and land use change: the conversion of temperate forests to avocado plantations and maize fields in central Mexico. Fungal Ecol 5:16–23

Hölker U, Höfer M, Lenz J (2004) Biotechnological advantages of laboratory-scale solid-state fermentation with fungi. Appl Microbiol Biotechnol 64:175–186. https://doi.org/10.1007/s00253-003-1504-3

Hubbe MA, Nazhad M, Sánchez C (2010) Composting as a way to convert cellulosic biomass and organic waste into high-value soil amendments: a review. BioResources 5:2808–2854

Husband R, Herre EA, Turner SL et al (2002) Molecular diversity of arbuscular mycorrhizal fungi and patterns of host association over time and space in a tropical forest. Mol Ecol 11:2669–2678. https://doi.org/10.1046/j.1365-294X.2002.01647.x

Jiménez D, Dini-Andreote F, van Elsas J (2014a) Metataxonomic profiling and prediction of functional behaviour of wheat straw degrading microbial consortia. Biotechnol Biofuels 7:92. https://doi.org/10.1186/1754-6834-7-92

Jiménez DJ, Korenblum E, van Elsas JD (2014b) Novel multispecies microbial consortia involved in lignocellulose and 5-hydroxymethylfurfural bioconversion. Appl Microbiol Biotechnol 98:2789–2803. https://doi.org/10.1007/s00253-013-5253-7

Leutritz J Jr (1946) A wood soil contact culture technique for laboratory study of wood-destroying fungi, wood decay and wood preservation. Bell Syst Tech J 25:102–135

Li L-L, McCorkle SR, Monchy S et al (2009) Bioprospecting metagenomes: glycosyl hydrolases for converting biomass. Biotechnol Biofuels 2:10. https://doi.org/10.1186/1754-6834-2-10

Liu Z, Wang Z, Sun J, Ni L (2020) The dynamics of volatile compounds and their correlation with the microbial succession during the traditional solid-state fermentation of Gutian Hong Qu

glutinous rice wine. Food Microbiol 86:103347. https://doi.org/10.1016/j.fm.2019.103347
Maaroufi NI, Nordin A, Palmqvist K et al (2019) Anthropogenic nitrogen enrichment enhances soil carbon accumulation by impacting saprotrophs rather than ectomycorrhizal fungal activity. Glob Chang Biol 25:2900–2914. https://doi.org/10.1111/gcb.14722
Madadi M, Abbas A (2017) Lignin degradation by fungal pretreatment: a review. J Plant Pathol Microbiol 8:1–6
McGuire KL, Zak DR, Edwards IP et al (2010) Slowed decomposition is biotically mediated in an ectomycorrhizal, tropical rain forest. Oecologia 164:785–795. https://doi.org/10.1007/s00442-010-1686-1
Montagnini F (2006) Homegardens of Mesoamerica: biodiversity, food security, and nutrient management. Tropical homegardens. Springer, Berlin, pp 61–84
Nguyen NH, Song Z, Bates ST et al (2016) FUNGuild: an open annotation tool for parsing fungal community datasets by ecological guild. Fungal Ecol 20:241–248. https://doi.org/10.1016/j.funeco.2015.06.006
Rivers AR, Weber KC, Gardner TG et al (2018) ITSxpress: software to rapidly trim internally transcribed spacer sequences with quality scores for marker gene analysis. F1000Research 7:1418
Sterkenburg E, Bahr A, Brandström Durling M et al (2015) Changes in fungal communities along a boreal forest soil fertility gradient. New Phytol 207:1145–1158
Tedersoo L, Bahram M, Põlme S et al (2014) Global diversity and geography of soil fungi. Science 346:1256688
UNITE Community (2019) UNITE QIIME release for eukaryotes. Version 18(11):2018
Vassileva M, Malusà E, Sas-Paszt L et al (2021) Fermentation strategies to improve soil bio-inoculant production and quality. Microorganisms 9:1254. https://doi.org/10.3390/microorganisms9061254
Voříšková J, Baldrian P (2013) Fungal community on decomposing leaf litter undergoes rapid successional changes. ISME J 7:477–486. https://doi.org/10.1038/ismej.2012.116
Yao H, He Z, Wilson M, Campbell CD (2000) Microbial biomass and community structure in a sequence of soils with increasing fertility and changing land use. Microb Ecol 40:223–237. https://doi.org/10.1007/s002480000053
Yurkov AM (2018) Yeasts of the soil–obscure but precious. Yeast 35:369–378
Zhang L, Zhang H, Wang Z et al (2016) Dynamic changes of the dominant functioning microbial community in the compost of a 90–m3 aerobic solid state fermentor revealed by integrated meta-omics. Bioresour Technol 203:1–10. https://doi.org/10.1016/j.biortech.2015.12.040
Zhang Q, Guo T, Li H et al (2020) Identification of fungal populations assimilating rice root residue-derived carbon by DNA stable-isotope probing. Appl Soil Ecol 147:103374